Relative stability of the $Al_{12}W$ structure in Al–transition-metal compounds

A. E. Carlsson
Department of Physics, Washington University, St. Louis, Missouri 63130
(Received 25 January 1991)

The structural stability of the prototypical complex $Al_{12}W$ structure, relative to the Cu_3Au structure, is computed for Al compounds with 3*d* and 4*d* transition metals. The calculated structural energy differences are on the order of an eV per transition-metal atom, have their largest negative magnitude for the transition metals with nearly half-filled *d* bands, and have larger magnitudes for the 4*d* transition metals than for the 3*d* metals. These results suggest that electronic effects are more important than atomic-size effects. It is shown that a large part of the structural energy differences is due to the presence of a Fermi-level nonbonding peak in the electronic density of states (DOS) for the Cu_3Au structure, which destabilizes that structure. The energy associated with the nonbonding peak has comparable contributions from a term in the energy that favors large unit-cell sizes, and from a local term that penalizes 90° bond angles around the transition-metal atoms. A significant additional contribution comes from the appearance of the dip in the DOS around the Fermi level for the $Al_{12}W$ structure. It is shown that the energetic factors developed here likely contribute to the relative stability of binary Al–transition-metal icosahedral phases.

I. INTRODUCTION

The discovery[1] of icosahedral (*i*) phases some six years ago in Al-rich transition-metal compounds has stimulated efforts[2–5] to understand the structures of the crystalline compounds at similar compositions. This is because the latter allow the underlying interatomic interactions to be studied in a better defined, more tractable environment than is provided by the *i* phases, and because it is believed[6] that the crystalline compounds may provide motifs which occur in the *i* phases as well. The latter contention is supported both by experimental scattering studies,[7–9] which show strong similarities between the local structures of the *i* phases and some crystalline structures, and by theoretical work[6,10] which has shown that models for the *i* phase can be obtained by continuously "deforming" observed crystalline structures, via a six-dimensional construction.

The "best" *i*-phase-forming Al-based systems are those having transition metals with roughly half-filled *d* bands, in columns VI–VIII of the Periodic Table. The crystalline structures formed by these compounds,[11] at Al-rich compositions, are complex in the sense of having large unit cells and point-group symmetry lower than cubic. Some of the structures having particularly large unit cells have been viewed as "rational approximants" to *i*-phase structures.[6,12] The complex crystal structures occur only over a narrow range of *d*-electron counts, with none of them occurring for transition metals in more than two columns of the Periodic Table. In addition, with the exceptions of Al_3Ru (which shares the Ni_3Ti structure with many transition-metal alloys) and the Al_6Mn structure, which is formed by As_6Ru, they occur only in Al– and Ga–transition-metal compounds.[11]

The most systematic study of the origins of the structures of this class of compounds has been performed via the "effective-medium" method.[2,3] Here the energy of a compound's crystal structure is determined by the energy of embedding the atomic constituents in a uniform electron gas with a density determined by the "background" density due to its neighbors. It was found that the icosahedral packing that occurs in some of the complex structures is associated with a preference of the transition-metal atom for high background electron density; this occurs at the icosahedral sites because the center-to-vertex distance of the icosahedron is 5% shorter than the vertex-to-vertex distance. These results were described in terms of a small *effective* atomic size for the transition-metal atom in the Al host, and thus provided *ab initio* support for atomic-size based theories of the structures of the Al–transition-metal alloys.

The effective-medium treatment in effect associates the transition-metal atoms with the electronic density of states (DOS) which they would have in a uniform electron gas of an appropriate density. Thus the overall width of the DOS is fairly accurate, but the detailed structure is probably not obtained correctly. The structure in the DOS has been studied in both cluster and bulk calculations. The cluster calculations[13] treated Mn atoms at the centers of 12- and 32-atom icosahedra. Both calculations showed a peak in the DOS at the Fermi level, which is expected to *destabilize* the icosahedral packing. The peak was attributed to the high symmetry of the icosahedral packing. This packing has no crystal-field splitting for *d* states, since in a spherical-harmonic decomposition of an icosahedral environment, the lowest-order nonzero contribution[14] is from $l=6$; *d*-state crystal-field splitting requires[15] $l \leq 4$. However, the conclusion drawn from the calculations would appear to be inconsistent with the stability of the $Al_{12}Mn$ compound, in which the Mn are icosahedrally coordinated by Al. Subsequent band-structure calculations[4] for the α-(Al-

Mn-Si) compound instead showed a dip in the DOS in the vicinity of the Fermi level. This was presumed to stabilize the α-(Al-Mn-Si) structure. In addition, there have been tight-binding calculations[16] using an underlying fcc lattice; for Al-rich alloys these showed a peak in the DOS around the Fermi level. On the basis of these results it was argued that there should be no stable, highly coordinated crystal structures for nearly half-filled transition-metal *d* bands.

However, at this point, the relative importance of the short-ranged interaction effects emphasized in the effective-medium-atom approach, and the electronic DOS effects, is not known. Furthermore, the precise origins of the various peaks and gaps near the Fermi level, and their connection with the long- and short-range orders, has not been established. Our aim is to treat some of these issues by performing a systematic series of *ab initio* structural stability calculations for Al-rich compounds of *all* of the 3*d* and 4*d* transition metals. We choose as a prototypical structural-energy different that between the $Al_{12}W$ and Cu_3Au structure. The $Al_{12}W$ structure[17] is chosen as a representative of the "complex" structures, and the Cu_3Au structure as a representative of the "simple" structures which one might imagine competing with the complex structures. The $Al_{12}W$ structure consists of a bcc array of Al icosahedra centered by transition-metal atoms, and thus contains 13 atoms per primitive unit cell. Thus it contains two important features which are characteristic of many of the complex structures, namely, a large unit cell and (partial) local icosahedral packing. The Cu_3Au structure, on the other hand, has all of the atoms residing on a fcc lattice, with the transition-metal atoms occupying a simple cubic sublattice containing a quarter of the sites. Thus each atom is surrounded by a cuboctahedron, and the primitive unit cell contains only four atoms.

We find that the structural energy differences are too large to be accounted for by atomic-size theories, and do not display the variation with transition-metal *d* count expected from these theories. Instead, the electronic structure around the Fermi level plays a major role. In those systems which favor the $Al_{12}W$ structure the most strongly, the competing Cu_3Au structure has a nonbonding peak in the DOS at the Fermi level, while the $Al_{12}W$ structure has a gap instead. We show, via a simple square-band model, that the elimination of the nonbonding peak in the $Al_{12}W$ structure leads to a stabilization energy comparable to the calculated *ab initio* structural energy difference. We investigate the origin of the nonbonding peak using an Anderson-lattice model. It results from the "sparseness" of plane-wave electron eigenfunctions in energy, which results from the small size of the unit cell. This effect is enhanced by high rotational symmetry. These factors are both present in the Cu_3Au structure, and are reduced in the $Al_{12}W$ structure. Thus there is a component of the energy which favors the complex structures *precisely because of their complexity,* rather than because of short-ranged packing constraints.

An additional component of the stabilization energy results from angular forces surrounding the transition-metal atom, which of course involve the potentials of the surrounding Al atoms. We investigate this effect via a tight-binding model of the DOS. An approximate solution of this model using a scheme based on the fourth and lower moments of the electronic DOS yields an angular force, for nearly half-filled band transition metals, which penalizes 90° bond angles. An analysis of the crystal structures formed by the nearly half-filled *d*-band transition metals shows that such bond angles are always absent for their Al-rich compounds.

The organization of the remainder of the paper is as follows. Section II briefly outlines the calculational method and presents the *ab initio* total-energy results and densities of states for the $Al_{12}W$ and Cu_3Au structures. Section III gives the model analyses, based on the square-band model, the Anderson-lattice model, and the tight-binding description. Section IV concludes the paper by describing the relevance of our results to icosahedral phases.

II. *ab initio* CALCULATIONS

Our *ab initio* calculations utilize the augmented-spherical-wave (ASW) method.[18] This is a fast linearized band-structure method based on the atomic-sphere approximation. The speed was necessary here, because of the size of the $Al_{12}W$ unit cell and the large number of calculations that were performed to ascertain the chemical trends. The approximations that are made in the ASW method are suitable for closely packed structures, such as the two that are treated here. Scalar relativistic effects are included as described in Ref. 19. Exchange and correlation effects are treated within the local-density approximation, implemented with a functional of the Hedin-Lundqvist form.[20] We present only non-spin-polarized results; spin-polarized calculations have been performed for the cases (groups-VI through group-VIII transition metals) where they should be largest, and they are always small (≤ 0.2 eV) in comparison with the scale of the calculated structural-energy differences. We used equal ASW sphere radii for all systems. In previous work we have found that this procedure yields alloy heats of formation which are in good agreement with experimental values for Al–transition-metal alloys and compounds;[21] in addition, the atomic-sphere approximation gives elemental structural-energy differences which are in good agreement with results from full-potential methods.[22]

For the Cu_3Au structure, the lattice constant was chosen which minimized the total energy. For the $Al_{12}W$ structure, the experimental lattice constants[11] were used where they have been measured (Mn, Mo, Tc). For the other systems, the lattice constants were obtained by interpolating or extrapolating the dependence of the observed lattice constants on the transition-metal atomic volume.

Figure 1(a) shows the calculated structural-energy difference:

$$\Delta E = E(Al_{12}T) - E(Al_3T) - 9E(Al) ,$$

where $Al_{12}T$ has the $Al_{12}W$ structure and Al_3T has the Cu_3Au structure. For the $Al_{12}W$ structure to form, it is

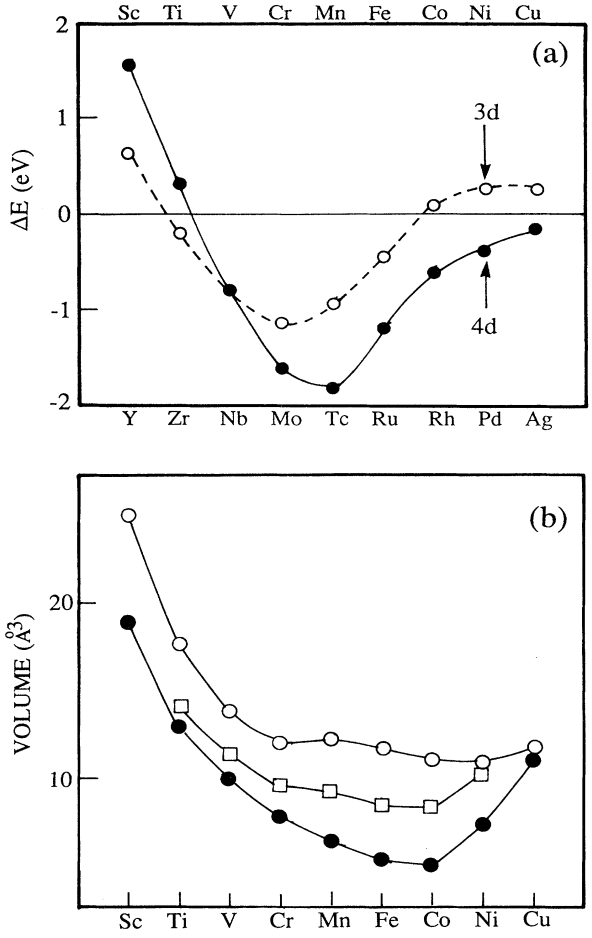

FIG. 1. (a) Energy difference between $Al_{12}W$ and Cu_3Au structures. Negative values indicate that $Al_{12}W$ is favored. (b) Atomic volumes for 3*d* transition metals. Open circles: elemental volumes taken from King (Ref. 25). Solid circles: effective sizes obtained from energy-minimization calculations for hypothetical Al_3T compounds. Squares: inverse of preferred electron density for transition-metal atoms in jellium, taken from K. Jacobsen, J. K. Nørskov, and M. J. Puska [Phys. Rev. B **35**, 7423 (1987)].

necessary (but not sufficient) that ΔE be negative; for the Cu_3Au structure to form with no $Al_{12}W$ structure phase at lower transition-metal concentrations, ΔE must be positive. The calculated values are consistent with the observed structures: Mn, Mo, and Tc form the $Al_{12}W$ structure, while Sc and Y form the Cu_3Au structure with no $Al_{12}W$ structure. In addition, the most negative values of ΔE in each row are found for the group-VI and group-VII transition metals, which form the $Al_{12}W$ structure. In cases for which ΔE is negative but the $Al_{12}W$ structure does not form, a third structure forms which has a lower energy than either of the two treated here. For example, Al_3Nb forms the $D0_{22}$ structure.[11] Its energy is estimated to be 0.8 eV to 1.0 eV per transition-metal atom below the $L1_2$ structure,[23,24] and thus slightly below that of the $Al_{12}W$ structure.

The main features of ΔE displayed in Fig. 1 are not sensitive to the choice of ASW sphere volumes. As a check on the accuracy of the equal-volume procedure, we have evaluated the structural-energy differences for a representative set of six compounds (Sc, Y, Cr, Tc, Ni, and Pd) using a complementary procedure which emphasizes atomic-size effects. (Cr and Tc are chosen as representative half-filled *d*-band transition metals because they have the largest negative values of ΔE). In this procedure the sphere radii are chosen to make each of the atomic spheres neutral, so that smaller atoms have smaller sphere volumes. For all of the metals except Ni, the effects on ΔE are less than 0.25 eV. Thus the large magnitude of the structural-energy differences is unaffected by the choice of sphere radii. The greater size of the values for the 4*d* row, relative to the 3*d* row, is also unaffected by the sphere radii. For Ni, ΔE is 0.57 eV more negative for the neutral-sphere method. However, even here the effect on the chemical trends is small. Comparing the numbers for Cr (0.22 eV more negative) and Ni, one finds that their difference is changed by 0.35 eV, which is only 25% of the difference in ΔE (1.42 eV) between these two systems.

Three aspects of the results are relevant to establishing the relative importance of effects due to effective atomic sizes and electronic effects.

(1) The large energy scale of ΔE. The largest value is for $Al_{12}Tc$ which has $\Delta E = -1.8$ eV. Since the replacement of the Tc by Al would cause ΔE to become positive

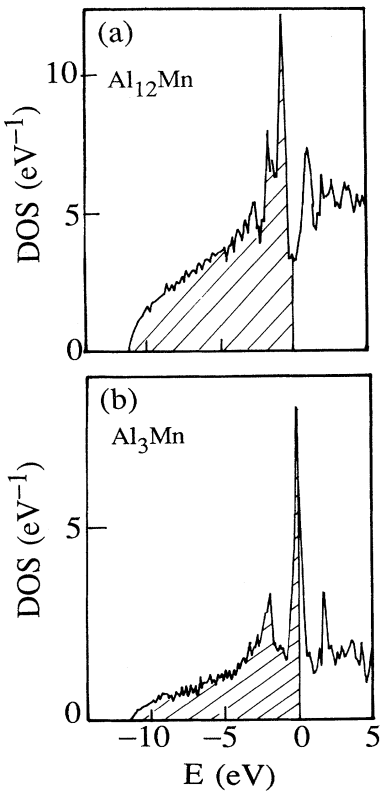

FIG. 2. Electron densities of states for (a) $Al_{12}Mn$ in $Al_{12}W$ structure and (b) Al_3Mn in Cu_3Au structure.

(since $Al_{12}W$ structure $Al_{12}Al$ does not form), this means that each Tc atom changes the structural energy by roughly 2 eV. In comparison, typical transition-metal structural energy differences are 0.5 eV per atom. The effective-medium calculations[3] mentioned in the Introduction yield a value of ΔE for Mn of only 0.1 eV versus the present value close to 1 eV.

(2) The characteristic dependence on transition-metal d count. For both the $3d$ and $4d$ transition metals, ΔE has its minimum at a roughly half-filled d band. For comparison we show in Fig. 1(b) elemental transition-metal atomic sizes,[25] as well as *effective* atomic sizes that we have obtained from the calculated Al_3T lattice constants.[26] In addition, atomic sizes derived from the preferred "background" electron densities[3] in the effective-medium method are shown. By each of these three measures, the atomic sizes have minima in groups VIII–X, significantly to the right of the minimum in ΔE. If atomic-size effects dominated, then ΔE should also have an inflection point (zero slope) at the minimum of the atomic sizes. Instead, at this minimum, ΔE is already rapidly climbing. Thus it is unlikely that the atomic size is the dominant effect driving the stability of the $Al_{12}W$ structure.

(3) The most negative values of ΔE occur in the $4d$ transition metals. If atomic size were the dominant factor, one would expect the $3d$ transition metals to have the most negative values of ΔE, since they have the smallest atomic sizes.

Thus the simplest theory, that based on effective atomic sizes, cannot explain the calculated structural-energy differences. The characteristic dependence of ΔE on the d-electron count suggests that electronic density-of-states (DOS) effects may be important. Typical DOS results, for the Al-Mn system, are shown in Fig. 2. In both the $Al_{12}W$ and $Cu_{13}Au$ structures, the parabola due to the Al nearly-free-electron states is clearly seen, along with a relatively narrow peak resulting from the Mn d states. In the Cu_3Au structure, the DOS contains a very high peak at the Fermi level. In the $Al_{12}W$ structure, this peak is split, and the DOS at the Fermi level is reduced relative to its free-electron value. We will show that the peak in the Cu_3Au structure DOS has a major impact on the value of ΔE. We will call it the "nonbonding" peak,

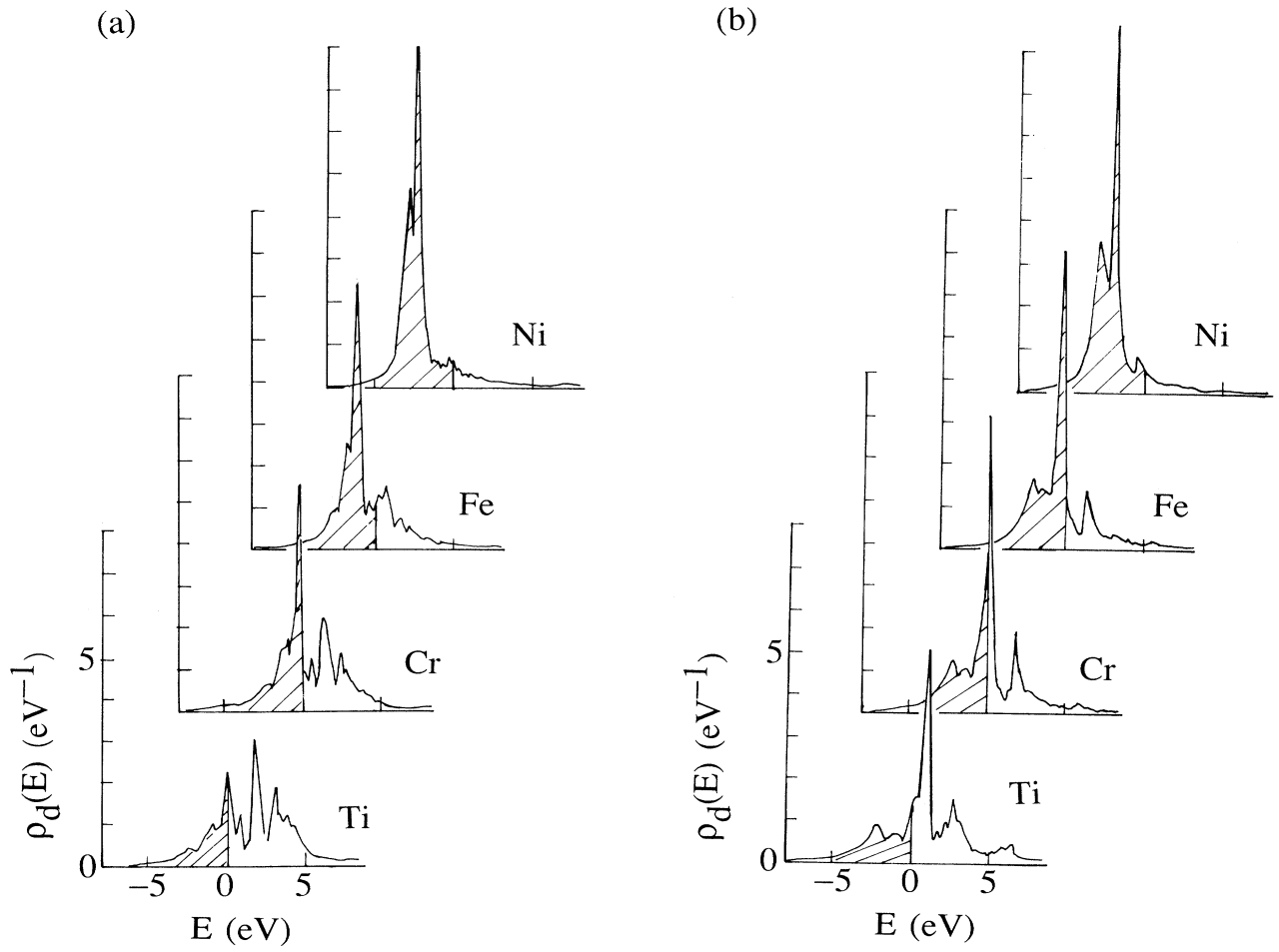

FIG. 3. Projected densities of states on transition-metal d orbitals for (a) $Al_{12}T$ compounds in $Al_{12}W$ structure and (b) Al_3T compounds in Cu_3Au structure.

deferring until later the demonstration that this is actually the origin of the peak. The chemical trends associated with the above features of the DOS are illustrated in Fig. 3, which shows the transition-metal d-projected DOS for $Al_{12}T$ and Al_3T compounds, for T=Ti, Cr, Fe, and Ni. As the d band goes from nearly empty (Ti) to nearly filled (Ni), the Fermi level passes smoothly through the nonbonding peak in the Cu_3Au structure, and the quasigap in the $Al_{12}W$ structure. The transition metals for which ΔE is the most negative are precisely those for which the Fermi level resides in the peak in the Cu_3Au structure DOS.

The calculated DOS distributions shown in Figs. 2 and 3 yield different physical pictures than are given in the cluster and tight-binding calculations. The cluster calculations[13] found an enhancement of the DOS at the Fermi level resulting from icosahedral packing, while our results for $Al_{12}Mn$ show exactly the opposite, a quasigap. The tight-binding calculations[16] had found, for the Al-Mn system, a narrow peak which was relatively structure independent. We find that the value of the DOS at the Fermi level depends very strongly on the structure. However, our results are consistent with the *ab initio* results[4] for the α-(Al-Mn-Si) structure, which had also found a reduction of the DOS near the Fermi level.

III. MODEL ANALYSES OF RESULTS

The *ab initio* results presented above, while arguing against effective atomic size as the dominant mechanism for stabilizing the $Al_{12}W$ structure, do not explicitly tell us which mechanisms are responsible. With this goal in mind we describe in this section three simplified models for analyzing the *ab initio* results. The first of these, a square-band model of the DOS, allows us to estimate the scale of the stabilization energy resulting from the absence of the nonbonding peak in the $Al_{12}W$ structure. The second model is an Anderson-lattice model for the transition-metal d shells, which explains the origin of the nonbonding peak. It allows us to assess the effects of the geometric arrangement of the transition-metal atoms in the Al host, temporarily ignoring the host's discrete atomic structure. The last model assesses the effects of the local packing of the Al atoms surrounding a particular transition-metal atom, via a tight-binding analysis.

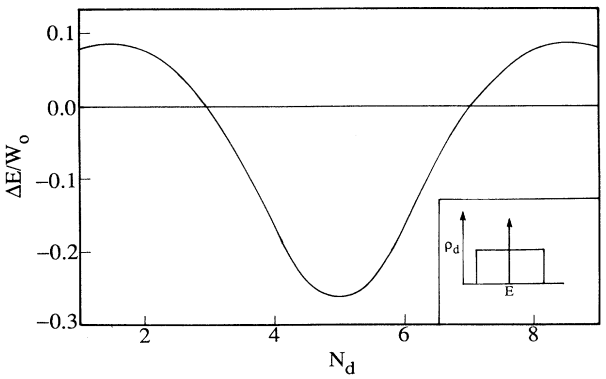

FIG. 4. Structural-energy difference for model density of states (cf. inset). N_d denotes d-band filling and W_0 is half-bandwidth for $f_p=0$.

A. Square-band model

On the basis of experience with many other systems, one expects that a peak of the type seen in the Cu_3Au DOS plots in Figs. 2 and 3 should provide a destabilizing contribution to the total energy, provided that the Fermi energy is in the peak. In other systems, such Fermi-surface effects can lead to[27] reduced rotational symmetry (the Jahn-Teller effect), a magnetic state, or a superconducting state. We will show that here, it contributes to the formation of structures with large unit cells and reduced rotational symmetry. To obtain a very simplified estimate of the magnitude of the peak contribution, we use the following model DOS (cf. inset, Fig. 4):

$$\rho_d(E)=\begin{cases}5(1-f_p)W^{-1}+10f_p\delta(E), & E<W\\ 0, & \text{otherwise.}\end{cases} \tag{1}$$

Here f_p is the weight factor for the nonbonding peak, at $E=0$. The electronic band energy for this DOS is readily computed. For $N_d<5$ one has

$$E_{\rm el}=\begin{cases}\int_{-\infty}^{\varepsilon_F}E\rho_d(E)dE=-N_dW[1-N_d(1-f_p)/10], & N_d<5(1-f_p) \quad (2a)\\ -\frac{5}{2}W(1-f_p), & N_d\geq 5(1-f_p). \quad (2b)\end{cases}$$

For $N_d\geq 5$ one uses Eqs. (2) together with the fact that $E_{\rm el}(N_d)=E_{\rm el}(10-N_d)$ for the even band considered here. We obtain the values of f_p in these expressions from Fig. 3, which shows that roughly two of the ten electrons that can be accommodated in the d band are contained in the nonbonding peak. Thus we choose $f_p=0.2$ for the Cu_3Au structure. For the $Al_{12}W$ structure we choose $f_p=0$, since the DOS at the Fermi level is actually *reduced* relative to its free-electron value (cf. Fig. 2). For calculating the structural energy differences, we choose values of W such that the second moment

$$\mu_2=\tfrac{1}{2}\int_{-\infty}^{\infty}E^2\rho_d(E)dE \tag{3}$$

is taken to be the same in both structures. (The factor of $\frac{1}{2}$ removes the spin degeneracy included in ρ_d). The motiva-

tion for this choice is to emphasize effects due to the *shape*[28] of the DOS, rather than its overall width as measured[29] by μ_2. The effects of changes in μ_2 are such as to favor one structure over the other at all band fillings. There is, in fact, precise justification[30] for calculating structural-energy differences at constant μ_2, provided that the differences in equilibrium volume per atom between the two phases are not too large. The μ_2 constraint implies that $(1-f_p)W^2=W_0^2$, where W_0 is the half-bandwidth for $f_p=0$. Thus Eqs. (2) become

$$E_{\rm el}=\begin{cases}-N_d W_0(1-f_p)^{-1/2}[1-N_d(1-f_p)/10], & N_d<5(1-f_p) \quad (3a)\\ -\frac{5}{2}W_0(1-f_p)^{1/2}, & N_d\geq 5(1-f_p). \quad (3b)\end{cases}$$

With the model thus specified we obtain the estimate of ΔE shown in Fig. 4. Here, the unit of energy is the half-bandwidth W for $f_p=0$. For values of W on the order of 3 eV for the 3*d* transition metals and 4 eV for the 4*d* metals, we obtain maximal values of ΔE of 0.75 eV for the 3*d* metals and 1.0 eV for the 4*d* metals. These values account for 60% or more of the *ab initio* values; the larger value of ΔE for the 4*d* metals is also consistent with the *ab initio* trends. Finally, ΔE has its largest value for a half-filled band, again consistent with the *ab initio* results. Thus the presence or absence of the nonbonding peak plays an important major role in determining ΔE.

B. Anderson-lattice model

The origin of the nonbonding peak can be established without taking into account the perturbations due to the Al pseudopotential. Thus we begin by studying the following Hamiltonian:

$$H=\sum_{\mathbf{k},\mathbf{K}}\varepsilon_{\mathbf{k}+\mathbf{K}}|\mathbf{k}+\mathbf{K}\rangle\langle\mathbf{k}+\mathbf{K}| +\varepsilon_d\sum_{\mathbf{k},m}|\mathbf{k},m\rangle\langle\mathbf{k},m| \times\sum_{\mathbf{k},\mathbf{K},m}(V_{\mathbf{k}+\mathbf{K},m}|\mathbf{k}+\mathbf{K}\rangle\langle\mathbf{k},m|+\text{H.c.}). \quad (4)$$

Here the $|\mathbf{k}+\mathbf{K}\rangle$ are plane waves with free-electron energies $\varepsilon_{\mathbf{k}+\mathbf{K}}$, $\mathbf{k}$ is in the first Brillouin zone, $\mathbf{K}$ is a reciprocal-lattice vector, $|m,\mathbf{k}\rangle=(1/N^{1/2})\sum_{\mathbf{R}}e^{i\mathbf{k}\cdot\mathbf{R}}|\mathbf{R},m\rangle$ is a *d*-orbital Bloch wave ($-2\leq m\leq 2$) with energy ε_d, and the $V_{\mathbf{k}+\mathbf{K},m}$ are *s*-*d* hybridization strengths. Here the $\mathbf{K}$ are the transition-metal sites and N is the number of transition-metal atoms. Direct *d*-*d* couplings are ignored, because the spacing between transition-metal atoms is large enough (≥ 3.7 Å) that indirect interactions mediated by the free-electron terms dominate. This follows from the $\mathbf{k}$ independence of ε_d since

$$\langle\mathbf{R},m|H|\mathbf{R}',m\rangle=\frac{\varepsilon_d}{N}\sum_{\mathbf{k}}e^{i\mathbf{k}\cdot(\mathbf{R}-\mathbf{R}')}=\varepsilon_d\delta_{\mathbf{R},\mathbf{R}'}. \quad (5)$$

To analyze the electronic structure of this Hamiltonian we begin with the case $V_{\mathbf{k}+\mathbf{K},m}=0$. In this case [cf. Fig. 5(a)], at each Bloch wave vector $\mathbf{k}$ in the first Brillouin zone, one has five eigenfunctions $|\mathbf{k},m\rangle$ in the *d* complex, as well as an infinite collection of plane waves at energies $\varepsilon_{\mathbf{k}+\mathbf{K}}$. When the *s*-*d* interactions $V_{\mathbf{k}+\mathbf{K},m}$ are "turned on," the energies of the *d*-wave functions are shifted by interaction with the plane waves. In degenerate second-order perturbation theory,[31] the energy shifts $\delta\varepsilon_d$ are equal to the eigenvalues of the matrix

$$\delta H^{\rm eff}_{m,m'}(\mathbf{k})=\sum_{\mathbf{K}}\frac{V^*_{\mathbf{k}+\mathbf{K},m}V_{\mathbf{k}+\mathbf{K},m'}}{(\varepsilon_d-\varepsilon_{\mathbf{k}+\mathbf{K}})}. \quad (6)$$

Thus the largest contributions to the *d*-energy shifts come from plane waves close in energy to ε_d. On the other hand, if a linear combination $|\psi_d\rangle=\sum_m C_m|\mathbf{k},m\rangle$ exists which does not couple to any plane waves with energies close to ε_d, the energy associated with this linear combination should only be shifted slightly. For a given $\mathbf{k}$ in the first Brillouin zone, consider the four reciprocal-lattice vectors $\mathbf{K}_1$, $\mathbf{K}_2$, $\mathbf{K}_3$, and $\mathbf{K}_4$ such that the energies $\varepsilon_{\mathbf{k}+\mathbf{K}}$ are closest to ε_d. By elementary linear algebra, the system of four equations in five unknowns

$$(\langle\mathbf{k}+\mathbf{K}|H|\psi_d\rangle)=\sum_m C_m V_{\mathbf{k}+\mathbf{K},m}=0, \quad i=1,2,3,4 \quad (7)$$

must have at least one nontrivial solution ψ_d. The shift $\Delta\varepsilon_d$, estimated as the expectation value $\langle\psi_d|\delta\hat{H}^{\rm eff}|\psi_d\rangle$,

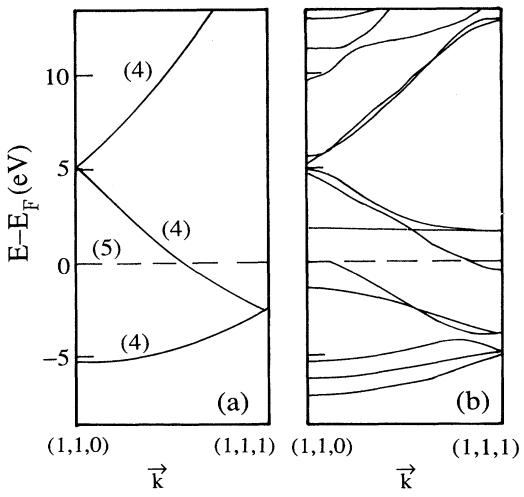

FIG. 5. (a) Free-electron band model for Al_3Mn in Cu_3Au structure at 3.80 Å lattice constant; dashed line denotes *d*-orbital energy. (b) *Ab initio* band structure for Al_3Mn in Cu_3Au structure.

will then be small because of the large energy denominators in Eq. (6).

Of course, there is no guarantee that $|\psi_d\rangle$ is an exact eigenfunction of the matrix $\delta\hat{H}^{\text{eff}}$. However, one can rigorously show that $\delta\hat{H}^{\text{eff}}$ must have a small eigenvalue associated with $|\psi_d\rangle$. To see this we apply the variational principle to $[\delta\hat{H}^{\text{eff}}]^2$. From Eqs. (6) one readily shows that

$$\langle\psi_d|\delta\hat{H}^{\text{eff}}(\mathbf{k})^2|\psi_d\rangle=\sum_{m,m',m'',\mathbf{K},\mathbf{K}'}\frac{C_m^*V_{\mathbf{k}+\mathbf{K},m}^*V_{\mathbf{k}+\mathbf{K},m''}V_{\mathbf{k}+\mathbf{K}',m''}^*V_{\mathbf{k}+\mathbf{K}',m}C_{m'}}{(\varepsilon_d-\varepsilon_{\mathbf{k}+\mathbf{K}})(\varepsilon_d-\varepsilon_{\mathbf{k}+\mathbf{K}'})}\ . \tag{8}$$

By Eq. (7) one need retain in Eq. (8) those reciprocal-lattice vectors $\mathbf{K}_i$ with $i\geq 5$. The variational principle for the lowest eigenvalue of a linear operator then implies that $\delta\hat{H}^{\text{eff}}(\mathbf{k})^2$ has an eigenvalue which is less than or equal to the right-hand side of Eq. (8). Since the eigenvalues of $\delta\hat{H}^{\text{eff}}(\mathbf{k})$ are the square roots of the eigenvalues of $\delta\hat{H}^{\text{eff}}(\mathbf{k})^2$, there is at least one eigenvector whose energy shift satisfies

$$|\delta\varepsilon_d|\leq\left|\sum_{m,m',\mathbf{K},\mathbf{K}'m,''}{}'\frac{C_m^*V_{\mathbf{k}+\mathbf{K},m}^*V_{\mathbf{k}+\mathbf{K},m''}V_{\mathbf{k}+\mathbf{K}',m''}V_{\mathbf{k}+\mathbf{K}',m'}C_{m'}}{(\varepsilon_d-\varepsilon_{\mathbf{k}+\mathbf{K}})(\varepsilon_d-\varepsilon_{\mathbf{k}+\mathbf{K}'})}\right|^{1/2}, \tag{9}$$

where the prime denotes that only $\mathbf{K}_i$ with $i\geq 5$ are included. The right-hand side of (9) is simply the norm $|\mathbf{u}|$ of the five-component vector whose mth component is

$$u_m=\sum_{m',\mathbf{K}}{}'\frac{V_{\mathbf{k}+\mathbf{K},m}^*V_{\mathbf{k}+\mathbf{K},m'}C_{m'}}{(\varepsilon_d-\varepsilon_{\mathbf{k}+\mathbf{K}})}\ .$$

Since $|\mathbf{C}|=(\sum_{m=1}C_m^2)^{1/2}=1$ it follows that $|\mathbf{u}|\leq\|\delta\hat{H}^{\text{eff},5}\|$, where

$$\delta\hat{H}^{\text{eff},5}_{m,m'}=\sum_{\mathbf{K}}{}'\frac{V_{\mathbf{k}+\mathbf{K},m}^*V_{\mathbf{k}+\mathbf{K},m'}}{(\varepsilon_d-\varepsilon_{\mathbf{k}+\mathbf{K}})} \tag{10}$$

and the norm $\|\ \|$ denotes the largest absolute value of the eigenvalues of an operator.

Thus at each value of $\mathbf{k}$, there is at least one state within an energy separation $\|\delta\hat{H}^{\text{eff},5}\|$ of the bare d-state energy ε_d. The width of the narrow band thus obtained depends on the energy denominators in Eq. (10), which in turn depend on the average energy splitting $\Delta\varepsilon$ between plane waves $|\mathbf{k}+\mathbf{K}\rangle$ that are neighboring in energy. The number of such plane waves per unit energy, at a particular Bloch wave vector $\mathbf{k}$ in the first Brillouin zone, should on the average be equal to the density of states per unit cell per spin. Thus an average value of $\Delta\varepsilon$ near the Fermi level should be

$$\Delta\varepsilon=2/\Omega\rho_{fe}(\varepsilon_F)\ , \tag{11}$$

where ρ_{fe} is simply the free-electron density of states; the factor of 2 accounts for the spin degeneracy in ρ_{fe}. Typically, the minimum energy difference $|\varepsilon_d-\varepsilon_{\mathbf{k}+\mathbf{K}}|$ in (10) would be $(5/2)\Delta\varepsilon$. Thus a reasonable value for the width of the narrow band is

$$W=\frac{2(|V_{\mathbf{k}+\mathbf{K},m}|)^2}{5\Delta\varepsilon}=\tfrac{1}{5}|V_{\mathbf{k}+K,m}|^2\Omega\rho_{fe}(\varepsilon_F)\ , \tag{12}$$

where $(|V_{\mathbf{k}+\mathbf{K},m}|)^2$ is a typical value of $|V_{\mathbf{k}+\mathbf{K},m}|^2$.

This effect is illustrated for the hypothetical Al_3Mn compound in Fig. 5(b), which shows the *ab initio* band structure for a lattice constant of 3.8 Å. For this case we have $\Delta\varepsilon=2$ eV from Eq. (11). By fitting the d-projected density of states similar to those shown in Fig. 3(b) to a Lorentzian shape, we obtain 1 eV as a typical value of $V_{\mathbf{k}+\mathbf{K},m}$. Thus we expect for the narrow band a width of roughly 0.2 eV, consistent with the calculated widths. The nonbonding effect is particularly large along the high-symmetry $(\pi/a,\pi/a,\eta)$ direction shown in Fig. 5. Along this direction, the 12 lowest-energy free-electron wave vectors have the form $\mathbf{k}+\mathbf{K}=(\pm\pi/a,\pm\pi/a,q)$. The small group of each vector $\mathbf{k}+\mathbf{K}$ has eight elements generated by 90° rotations about the z axis, and reflection through the x and y axes. The (x^2-y^2) d orbital belongs to the representation which is odd under the 90° rotations but even under the reflections, while the plane waves $\mathbf{k}+\mathbf{K}$ belong to other representations. Therefore the (x^2-y^2) d orbital couples to none of these plane waves, leading us to expect an extremely narrow band; this is confirmed by the calculated band structure, which shows a bandwidth of less than 0.1 eV in the direction plotted. Thus the large nonbonding peak is due to both the *small real-space unit cell,* which leads to a large value of $\Delta\varepsilon$ [cf. Eq. (11)], and the *high point-group symmetry,* which further eliminates possible *s-d* couplings.

Both of these contributing factors are reduced in the $Al_{12}W$ structure. The unit-cell size is more than three times larger than that of the Cu_3Au structure, which gives $\Delta\varepsilon\approx 0.6$ eV. The rotational symmetry is reduced, because the fourfold axes in the cubic group of the Cu_3Au structure become twofold axes in the reduced group of the $Al_{12}W$ structure. We then expect to see a much smaller density of states in the region within a few tenths of an eV of the band center, as is seen in Fig. 3(a).

Thus compounds of Al with transition metals in columns VI and VII should be stabilized by large unit-cell size and low point-group symmetry. Both of the factors are present in all of the observed crystal structures. All of them have at least 12 atoms per unit cell, and in most cases symmetry lower than cubic. In fact, with the exception of the $Al_{12}W$ and α-(Al-Mn-Si) structure com-

pounds, the symmetry is tetragonal or lower.

Additional support for the stabilizing mechanism discussed above comes from the previously mentioned *ab initio* electronic-structure calculations[4] for the α-(Al-Mn-Si) structure. These showed a dip in the density of states in the vicinity of the Fermi level. In addition, the experimentally observed[32] absence of magnetic moments on Mn in the α-(Al-Mn-Si) and Al_6Mn structures suggests that they have a reduced Fermi-level state density. Finally, we note that a somewhat similar mechanism seems to operate in stabilizing transition-metal alloy complex phases as well.[5,33] In comparison with the fcc structure, these complex phases have a reduced average density of states in a relatively broad region around the Fermi level. However in the transition-metal alloy case, the fcc structure does not display nearly as sharp a peak such as the one seen here. This is probably because in the purely transition-metal case, there is a larger density of d states available for hybridization.

For the purposes of modeling the Al-rich transition-metal compounds and alloys, it is useful to establish the relative importance of the two factors discussed above, unit-cell size and reduced point-group symmetry. We have made some progress in this direction by considering a hypothetical $Al_{15}T$ structure in which the atoms occupy the sites of a fcc lattice, and the transition-metal atoms T are arranged on a bcc lattice. This structure has the large unit-cell effect, but not the reduced point-group symmetry. Thus the energy difference

$$\Delta\tilde{E}=E(Al_{15}T)-E(Al_3T)-12E(Al)$$

should indicate the importance of the unit-cell size effect. We have calculated this energy difference for the transition metals with nearly half-filled d shells. The lattice constant corresponding to the minimum energy for the Cu_3Au structure was used for each of the three calculations entering $\Delta\tilde{E}$. The energy differences are given in Table I. For the group-VI and -VII metals, $\Delta\tilde{E}$ corresponds to 30–50% of the nonbonding peak contribution as estimated from Eq. (2), or 20–30% of the $Al_{12}W$ versus Cu_3Au energy difference. For the group-V and -VIII transition metals, the unit-cell size effect appears to be practically negligible. Thus, in these cases a large part of the effects of the nonbonding peak comes from other causes, such as the symmetry of the local environment. To treat this effect, one could include the effects of the Al pseudopotential by adding perturbing terms to Eq. (4). At present, we see no straightforward way of treating the effects of these terms. Therefore, we defer discussion of the local-environment effect to the next subsection which evaluates them within a tight-binding context.

TABLE I. Energy difference $\Delta\tilde{E}$ between hypothetical $Al_{15}T$ compound and combination of Al_3T and Al.

T	$\Delta\tilde{E}$
Cr	−0.33 eV
Mn	−0.34 eV
Mo	−0.29 eV
Tc	−0.48 eV

C. Tight-binding model

The effects of the symmetry of the transition-metal local environment are most easily explored via a tight-binding analysis. The characteristic angular dependences of the relevant wave functions are immediately apparent in the Hamiltonian, and can be directly translated[5,28] into angular forces which discriminate between various possible local environments. As a basis set, we use the d orbitals on the transition-metal sites, and s and p orbitals on the Al sites. This gives a Hamiltonian of the following form:

$$H=\sum_{i,\mu}\varepsilon_{i,\mu}|i,\mu\rangle\langle i,\mu|+\sum_{ij,\mu\nu}h_{ij}^{\mu\nu}|i,\mu\rangle\langle j,\nu| \ . \tag{13}$$

Here i and j denote atomic sites; μ and ν are orbital indices which describe s and p orbitals on Al sites and d orbitals on transition-metal sites. Here the $\varepsilon_{i,\mu}$ are single-site energies which on transition-metal sites have the value ε_d, and on Al sites have the values ε_s or ε_p. The $h_{ij}^{\mu,\nu}$ are interatomic couplings whose angular dependence is determined by the Slater-Koster relations[34] for two-center integrals. We will, for simplicity, focus on the effects of only the σ couplings. For our analysis, which focuses on the effects of changes in the angular environment, rather than on the effects of the local *density* of neighbors, it will not be necessary to specify the form of the radial dependence of the couplings. The results will depend only on the Slater-Koster relations and estimates of the d-band width.

Our analysis of the angular forces is based on a moment analysis of ρ_d, the DOS projected on a transition-metal d orbital. The moments are defined by

$$\mu_n=\tfrac{1}{2}\int_{-\infty}^{\infty}(E-\varepsilon_d)^n\rho_d(E)dE \ ,$$

where the factor of $\frac{1}{2}$ "undoes" the spin degeneracy contained in ρ_d. For example, $\mu_0=5$ and, as mentioned above, μ_2 describes the average width of the d complex. In Sec. III A it was found that the calculated structural-energy differences depended strongly on the contribution of the nonbonding peak at roughly the center of the d band. The lowest-order moment that describes it is[28] μ_4. It may be thought of as describing fluctuations in E^2, and is thus minimized (at fixed μ_2) for a bimodal DOS having only two δ functions with equal weights. For DOS having large contributions at the center of the band, as well as in its outer regions, μ_4 is larger. A small value of μ_4 typically results in a reduced DOS at the Fermi level. If all lower moments are equal, this is preferred for bands which are nearly half-filled.[35] For nearly filled or empty bands, a large value of μ_4 is preferred, since such a DOS has broader tails.

The connection between μ_4 and the angular forces is based on the rigorous real-space formulation[36] of μ_4:

$$\mu_4(i)=\sum_{\mu}\sum_{j,k,l}\sum_{\nu,\eta,\xi}h_{ij}^{\mu\nu}h_{jk}^{\nu\eta}h_{kl}^{\eta\varepsilon}h_{li}^{\varepsilon\mu} \ , \tag{14}$$

where $\mu_4(i)$ corresponds to the projected DOS on site i. Our main concern will be with the self-retracing paths in which the second hop leads back to the transition-metal

atom. We will denote this part of μ_4 by

$$\mu_4^{(2)}(i)=\sum_{\mu}\sum_{j,k}\sum_{\nu,\eta,\xi} h_{ij}^{\mu\nu}h_{ji}^{\mu\nu}h_{ik}^{\eta\xi}h_{ki}^{\xi\mu} . \quad (15)$$

The local angular environment influences $\mu_4^{(2)}$ via the angular dependence of the hopping integrals. Since the electronic-band energy depends on μ_4, and μ_4 in turn depends on the local angular geometry, one can derive[5,28,37] a connection between this geometry and the band energy. This connection is based on linearizing the dependence of the band energy on μ_4, and takes the form of an angular three-body effective potential:

$$V_3^{\rm eff}(i,j,k)=\mu_4^{(2)}(ijk)\frac{\partial E_{\rm el}}{\partial\mu_4} , \quad (16)$$

where the derivative is taken at fixed μ_2 and i is the transition-metal site. The normalization of $V_3^{\rm eff}$ is such that the structural energies per transition-metal atom i have the form $\sum_{j,k}V_3^{\rm eff}(i,j,k)$. In Eq. (16)

$$\mu_4^{(2)}(ijk)=\sum_{\mu,\nu,\eta,\xi} h_{ij}^{\mu\nu}h_{ji}^{\nu\eta}h_{jk}^{\eta\xi}h_{kl}^{\eta\mu} \quad (17)$$

is the contribution to $\mu_4^{(2)}(i)$ from the path through j and k, and the derivative $\partial E_{\rm el}/\partial\mu_4$ is obtained from a model DOS with parameters which are adjusted to obtain the correct moments. The derivative is evaluated in a reference environment, which we choose to be the icosahedral one ($f_p=0$); using a cubic reference environment changes strength of the potential by only 10%. We use the model DOS used above [cf. Eq. (1)] to describe the effects of the nonbonding peak. This gives the following dependence of f_p on μ_2 and μ_4:

$$f_p=1-\frac{9}{5}\left[\frac{\mu_2^2}{\mu_4\mu_0}\right] . \quad (18)$$

Here $\mu_0=5$ is the total weight of the band. From Eqs. (3b) and (18), using the chain rule for derivatives, we obtain for a half-filled band ($N_d=5$)

$$\frac{\partial E_{\rm el}}{\partial\mu_4}=\frac{\partial E_{\rm el}}{\partial f_p}\frac{\partial f_p}{\partial\mu_4}=\tfrac{9}{4}W\mu_2^2/(\mu_4^2\mu_0) .$$

We note that $W=\sqrt{3\mu_2/\mu_0}$; thus we obtain $\partial E_{\rm el}/\partial\mu_4=9/4\sqrt{3}\,\mu_2^{5/2}/\mu_4^2\mu_0^{3/2}$. Finally, one can show that if only σ couplings are kept, then $\mu_4^{(2)}(ijk)$ has[38] a simple analytical form

$$\mu_4^{(2)}(ijk)=h_{ij,\sigma}^2h_{ik,\sigma}^2[P_2(\cos\theta_{ijk})]^2 ,$$

where θ_{ijk} is the angle between the ij and ik bonds. Thus we obtain the following expression for the three-body interaction:

$$V_3^{\rm eff}(ijk)=\tfrac{9}{4}\sqrt{3}[P_2(\cos\theta_{ijk})]^2(h_{ij,\sigma}^2h_{ik,\sigma}^2)\mu_2^{5/2}/(\mu_4^2\mu_0^{3/2}) . \quad (19)$$

For Al-Mn, taking $W_0=3$ eV as in Sec. III A, we have $(\mu_2/\mu_0)=3$ eV^2; for $f_p=0$ (the reference-environment value), $(\mu_2^2/\mu_4\mu_0)=0.55$ from (18). If nearest-neighbor interactions are assumed to dominate μ_2, the $h_{ij,\sigma}^2=\frac{1}{12}\mu_2$ for all j. Assembling these values, and recalling that $\mu_0=5$, we obtain from Eq. (19) that $V_3^{\rm eff}(ijk)=(0.072$ eV$)[P_2(\cos\theta)]^2$.

$V_3^{\rm eff}$ is plotted in Fig. 6. The most important feature of this interaction is the peak at 90°; minima are seen at 55° and 125°. As shown in Figs. 6(b) and 6(c), the peak at 90° makes a contribution that favors the $Al_{12}W$ structure over the Cu_3Au structure. The contribution of the angular interaction to the structural-energy difference is found to be 0.20 eV per Mn atom, which accounts for roughly 30% of the contribution of the nonbonding peak. Thus this effect is somewhat smaller than the unit-cell size effect discussed above.

Geometric analysis of other observed structures of Al compounds with group-VI and -VII transition metals supports the presence of an angular potential which penalizes 90° bond angles around the transition-metal atoms. Histograms of the bond angles present in the α-(Al-Mn-Si) and Al_6Mn structures[17] are shown in Fig. 7. Few bond angles within 15° of 90° are seen. In comparison, the Cu_3Au structure, which is formed by Al_3Sc and Al_3Y, but not by the group-VI and group-VII compounds, has many such bond angles. The latter transition metals, such as Co and Ni, form structures[17] with bond angles which are not precisely 90°, but are closer to 90°

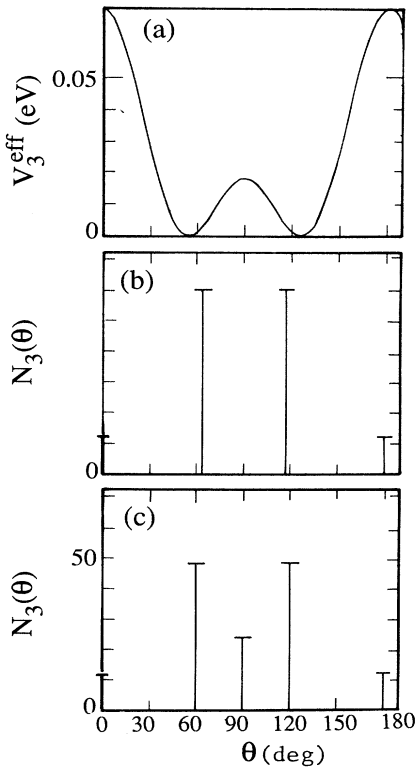

FIG. 6. (a) Angular three-body potential for Mn in Al. Al-Mn-Al bond angle denoted by θ. (b) Bond-angle distribution of transition-metal environment in $Al_{12}W$ structure. $N_3(\theta)$ denotes number of Al-Mn bond pairs, separated by angle θ, surrounding Mn site. (c) Bond-angle distribution of transition-metal environment in Cu_3Au structure Al_3T compounds.

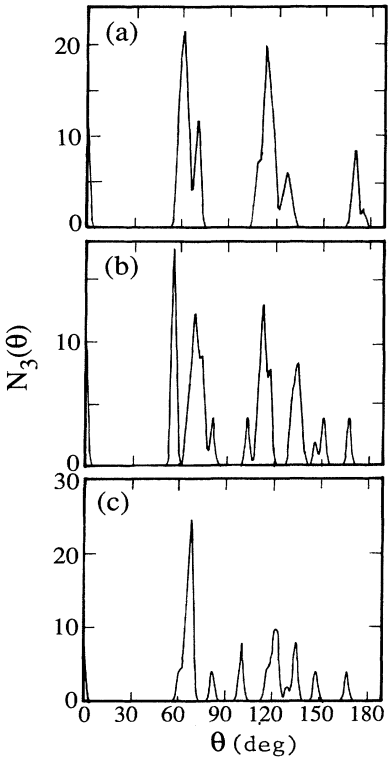

FIG. 7. Bond-angle distribution of transition-metal environment for (a) icosahedron center Mn site in Al-Mn-Si, (b) icosahedron Mn vertex site in Al-Mn-Si, and (c) Mn site in Al_6Mn. $N_3(\theta)$ is broadened to simplify visualization of distribution.

than those of the group-VI and -VII transition metal compounds.

D. Other contributions

The factors which we have treated so far account, in combination, for roughly 50% of the *ab initio* structural-energy differences. We cannot establish at this point whether we have underestimated the effects of these factors, or other factors make significant contributions. We have not treated radial factors such as those included in the "effective-medium" calculations[2,3] discussed above. It is possible that these are larger than the "effective-medium" estimates. Since these estimates are based on a uniform electron gas, they presumably do not completely account for the covalent-bonding effects which must be present in the Al–transition-metal interaction. In addition, the presence of the quasigap in the Fermi-level DOS in the *ab initio* calculations may make a large contribution (beyond the elimination of the nonbonding peak). The integrated reduction in weight due to the quasigap amounts to roughly two electrons, or approximately the same as the weight of the nonbonding peak. This would suggest a contribution of the same magnitude as that of the nonbonding peak. However, we do not at present have a theory describing the origin of the quasigap, and we cannot give a real-space formulation of the stabilization energy associated with it.

IV. CONCLUSIONS: RELEVANCE TO ICOSAHEDRAL PHASES

So far we have isolated some of the energetic factors which are responsible for the stabilization of the $Al_{12}W$ structure in Al–transition-metal compounds. We will conclude this paper by speculating on the importance of these factors in icosahedral (*i*) phases. The behavior of the DOS near the Fermi level, which we have emphasized in our analysis, appears to be an important factor in the formation of quasicrystals[39–41] and in discriminating between stable and metastable quasicrystals. The latter conclusion is based on electronic specific-heat measurements[42] of nearly-free-electron *i* phases, which found that stable *i* phases have much lower values of the DOS at the Fermi level than metastable ones. Our analysis suggests that the *i* phase, with its lack of both translational and rotational symmetry (at most a finite number of sites actually have strictly icosahedral symmetry), should have a lower Fermi level DOS than simple competing structures with cubic symmetry, such as the Cu_3Au structure, if the *d* band is nearly half-filled. This should provide a stabilizing contribution for the *i* phase. The observation that binary Al–transition-metal *i* phases form most easily for transition metals with nearly-half-filled *d* bands supports this contention. As a caution, however, we note that the above energy terms do not appear to be *necessary* for the formation of *i* phases, which can form[43] even with the late transition metals, where these terms are less important, and may even change sign.

In addition to illuminating the stability of *i* phases, the present results also have implications for their structure. Nuclear magnetic resonance[32] and magnetic susceptibility[44] measurements for the Al-Mn *i* phase have suggested a distribution of magnetic moments on the Mn sites. On the basis of the Stoner theory of magnetism, this should be associated with a distribution of values of the DOS at the Fermi level (in a preceding paramagnetic state). According to the results of Sec. III C, such a distribution might be due to a distribution of local site geometries. For example, those having symmetry close to cubic might be expected to have higher values of the DOS, and others to have lower values. Broad distributions of Mn site geometries are certainly present in all existing models of the *i* phase. Of course, variations in the local density of Al atoms surrounding the Mn atoms would also lead to variations in the Fermi-level DOS. At present we see no way to experimentally distinguish between the angular effect and the local-density effect.

It would be desirable to include the types of terms discussed in Sec. III in atomistic simulations of quasicrystals and their formation. Most existing simulations of rapidly quenched structures have relied on radial interaction.[14,45,46] Even at this level, it has been argued that a measure of local icosahedral packing is naturally present in undercooled liquids. Here we have seen that angular forces couple very strongly to various types of local structures which could be found in such liquids; their effect on

local icosahedral packing may well be larger than those of the radial terms. Also, since the sign of the angular terms varies fairly rapidly across a transition-metal row, angular forces should be very useful in studying chemical trends in liquid and quasicrystal structure. In the absence of *ab initio* schemes for handling these systems, the study of such trends is likely the most profitable way of obtaining an understanding of the metastability and stability of *i* phases.

ACKNOWLEDGMENTS

I am grateful to Art Williams and Victor Moruzzi for supplying me with the augmented-spherical-wave code developed at IBM, and to Jurgen Kübler for the use of his relativistic corrections to that code. I appreciate useful conversations with Andrew Zangwill and Rob Phillips. This work was supported by the United States Department of Energy under Grant No. DE-FG02-84ER45130.

[1]D. S. Shectman, I. Blech, D. Gratias, and J. W. Cahn, Phys. Rev. Lett. **53**, 1951 (1984).

[2]A. C. Redfield and A. Zangwill, Phys. Rev. Lett. **58**, 2322 (1987).

[3]A. Zangwill and A. C. Redfield, J. Phys. F **18**, 1 (1988).

[4]T. Fujiwara, Phys. Rev. B **40**, 942 (1989).

[5]R. B. Phillips and A. E. Carlsson, Phys. Rev. B **42**, 3345 (1990).

[6]V. Elser and C. L. Henley, Phys. Rev. Lett. **55**, 2883 (1985).

[7]Y. Ma and E. A. Stern, Phys. Rev. B **38**, 3754 (1988).

[8]J. W. Cahn, D. Gratias, and B. Mozer, Phys. Rev. B **38**, 1638 (1988).

[9]L. E. Levine, J. C. Holzer, P. C. Gibbons, and K. F. Kelton, Bull. Am. Phys. Soc. **35**, 330 (1990); L. E. Levine, Ph.D. thesis, Washington University, 1990 (unpublished).

[10]C. L. Henley and V. Elser, Philos. Mag. B **53**, L59 (1986).

[11]See P. Villars and L. D. Calvert, *Pearson's Handbook of Crystallographic Data for Intermetallic Phases* (ASM, Metals Park, Ohio, 1986).

[12]A useful collection of articles may be found in *The Physics of Quasicrystals,* edited by P. J. Steinhardt and S. Ostlund (World Scientific, New Jersey, 1987).

[13]M. E. McHenry, M. E. Eberhart, R. C. O'Handley, and K. H. Johnson, Phys. Rev. Lett. **56**, 81 (1986).

[14]P. J. Steinhardt, D. R. Nelson, and M. Ronchetti, Phys. Rev. B **28**, 784 (1983).

[15]This follows from the standard rules for addition of angular momentum, which imply that the product of two *d* orbitals ($l=2$) contains only components with $l \leq 4$.

[16]E. Voisin and A. Pasturel, Philos. Mag. Lett. **55**, 123 (1987).

[17]W. B. Pearson, *The Crystal Chemistry and Physics of Metals and Alloys* (Wiley, New York, 1972).

[18]A. R. Williams, J. R. Kübler, and C. D. Gelatt, Phys. Rev. B **19**, 6094 (1979).

[19]M. Methfessel and J. R. Kübler, J. Phys. F **12**, 141 (1982).

[20]L. Hedin and B. I. Lundqvist, J. Phys. C **4**, 2064 (1971).

[21]A. E. Carlsson, Phys. Rev. B **40**, 912 (1989).

[22]G. W. Fernando, R. E. Watson, M. Weinert, Y. J. Wang, and J. W. Davenport, Phys. Rev. B **41**, 11 813 (1990).

[23]A. E. Carlsson and P. J. Meschter, J. Mater. Res. **4**, 1060 (1989).

[24]J-H. Xu and A. J. Freeman, Phys. Rev. B **40**, 11 927 (1989).

[25]See H. W. King, in *Physical Metallurgy,* edited by R. W. Cahn and P. Haasen (North-Holland, New York, 1983), Chap. 2, Table V.

[26]The sizes are obtained on the assumption that the volume of the Al_3T compound is given as the composition-weighted average of the elemental Al volume and the effective transition-metal volume.

[27]C. Kittel, *Introduction to Solid State Physics* (Wiley, New York, 1986).

[28]A. E. Carlsson, in *Solid State Physics: Advances in Research and Applications,* edited by H. Ehrenreich and D. Turnbull (Academic, New York, 1990), Vol. 43, p. 1.

[29]For a discussion, see V. Heine, in *Solid State Physics: Advances in Research and Applications,* edited by H. Ehrenreich, F. Seitz, and D. Turnbull (Academic, New York, 1980), Vol. 35, p. 1.

[30]D. G. Pettifor and R. Podloucky, Phys. Rev. Lett. **53**, 1080 (1984).

[31]See L. D. Landau and E. M. Lifshitz, *Quantum Mechanics (Non-Relativistic Theory),* 3rd ed. (Pergamon, New York, 1977), Chap. VI, Sec. 39.

[32]W. W. Warren, Jr., H. S. Chen, and G. P. Espinosa, Phys. Rev. B **34**, 4902 (1986).

[33]P. Turchi, G. Treglia, and F. Ducastelle, J. Phys. F **13**, 2543 (1983).

[34]J. C. Slater and G. F. Koster, Phys. Rev. **94**, 1498 (1954). These are conveniently summarized in W. Harrison, *Electronic Structure and the Properties of Solids* (Freeman, San Francisco, 1980), Chap. 20.

[35]P. Turchi and F. Ducastelle, in *The Recursion Method and Its Applications,* edited by D. Pettifor and D. L. Weaire (Springer, New York, 1985), p. 104.

[36]F. Cyrot-Lackman, J. Phys. Chem. Solids **29**, 1235 (1968).

[37]A. E. Carlsson, Phys. Rev. B **32**, 4866 (1985).

[38]K. Hirai and J. Kanamori, J. Phys. Soc. Jpn. **50**, 2265 (1981).

[39]A. P. Smith and N. W. Ashcroft, Phys. Rev. Lett. **59**, 1365 (1987).

[40]J. Friedel, Helv. Phys. Acta **61**, 538 (1988).

[41]V. G. Vaks, V. V. Kamyshenko, and G. D. Samolyuk, Phys. Lett. A **132**, 131 (1988).

[42]J. L. Wagner, J. M. Wong, and S. J. Poon, Phys. Rev. B **39**, 8091 (1989).

[43]R. A. Dunlap and K. Dini, J. Phys. F **16**, 11 (1986).

[44]M. Eibschutz, M. E. Lines, H. S. Chen, and J. V. Waszczak, Phys. Rev. B **38**, 10 038 (1988).

[45]P. J. Steinhardt, D. R. Nelson, and M. Ronchetti, Phys. Rev. Lett. **47**, 1297 (1981).

[46]H. Jonsson and H. C. Andersen, Phys. Rev. Lett. **60**, 2295 (1988).